14,01

Effect of annealing on mechanical, elastic and microplastic properties of aluminum alloy AD1 in various structural states

© M.V. Narykova, B.K. Kardashev, A.A. Levin, A.G. Kadomtsev, V.I. Betekhtin, A.I. Lihachev

Ioffe Institute,
St. Petersburg, Russia

E-mail: Maria.Narykova@mail.ioffe.ru

Received April 9, 2024
Revised April 9, 2024
Accepted May 3, 2024

The work studied the effect of isothermal annealing in the temperature range 50−300°C on the structure, microhardness, elastic and microplastic properties of aluminum alloy AD1 in various structural states. Structure studies were carried out using electron backscatter diffraction, transmission electron microscopy, X-ray diffraction and densitometry. A temperature range has been determined that ensures the stability of the above characteristics of the AD1 alloy.

Keywords: aluminum AD1, elastic modulus, Young's modulus, ultrafine-grained aluminum, microhardness, microcrystalline aluminum, decrement.

DOI: 10.61011/PSS.2024.06.58714.83

1. Introduction

The technical aluminum AD1 belongs to deformable alloys, the high corrosion resistance of which allows for a broad application of this alloy in various fields of industry. The formation of an ultra-fine grain (UFG) state by various methods based on severe plastic deformation can significantly improve the strength characteristics of materials [1–3]. However, the increase of the strength by creating a UFG state requires the study of the grain structural stability and mechanical properties not only at the formation stage, but also during operation, which can take place at elevated temperatures. Therefore, the study of the temperature range that ensures the stability of the structure and properties of ultra-fine grain metallic materials is relevant.

This work continues the study in Ref. [4] of UFG of AD1 aluminum. This study analyzes the results for AD1 aluminum samples in various structural states, first obtained using a technology combining helical and longitudinal rolling and successfully used to form a UFG structure in titanium [5].

2. Samples and methods of study

The study was carried out on technical aluminum of grade AD1 which contains up to 0.3 wt.% Fe, up to 0.3 wt.% Si, up to 0.15 wt.% Ti, up to 0.1 wt.% Zn, up to 0.05 wt.% Cu, up to 0.05 wt.% Mg, up to 0.025 wt.% Mn and up to 0.05 wt.% of other impurities according to the datasheet. Two submicrocrystalline states were formed in the mechanical-thermal treatment mode [5], designated as SMC-1 and SMC-2. After rolling, the bars had the shape of a rod of circular cross-section with a diameter of approximately 7 mm. The process of formation of submicrocrystalline structures for these states differed in the temperature during finishing rolling: SMC-1 was carried out at room temperature, SMC-2 was carried out using the additional cooling in liquid nitrogen. A recrystallized microcrystalline (hereinafter denoted as MC) state was formed from SMC-1 by annealing at a temperature of 250°C for one hour.

A series of isothermal annealings was carried out in the range 50−350°C with a step of 50°C for a duration of 45 min to 4 h (for temperature 200°C) in a furnace SNOL 6.7/1300 for studying the thermal stability of the structure and mechanical properties.

The studies of the grain structure of the samples were carried out using a JSM 7001F scanning-electron microscope (JEOL, Japan) equipped with an HKL Nordlys EBSD detector (Oxford Instruments, England). Maps of crystallographic orientations of grains were obtained using the electron back-scattered diffraction (EBSD) method, grain size distributions and grain boundaries by disorientation angles were constructed. The samples were prepared by mechanical grinding of the surface using grinder Multi Prep 8 (Allied, San Francisco, CA, USA), followed by finishing polishing with a wide beam of argon ions using 1061 SEM Mill (Fischione, Export, PA, USA).

X-ray diffraction (XRD) studies were carried out using D2 Phaser powder X-ray diffractometer (Bruker AXS, Karlsruhe, Germany) in the Bragg–Brentano geometry using doublet CuK_α radiation from an X-ray tube with a copper anode, filtered using an CuK_β filter in the form of Ni-foil. A semiconductor linear X-ray detector LYNXEYE (Bruker AXS) was applied to record XRD patterns. The temperature in the sample chamber in the diffractometer was 41 ± 1°C during the measurement pro-

cess. The measurements were performed in the symmetric scanning mode $\theta-2\theta$. X-ray diffraction analysis of the measured diffraction patterns was performed using the EVA program (version 5.1.0.5) [6] with the powder database PDF-2 [7]. The EVA program was also used to obtain the parameters of the observed reflections which were used for calculation of the structural and microstructure parameters. The parameters of the Al cubic unit cell for the samples was calculated from the measured Bragg angles $2\theta_B$ of the observed reflections after introducing angular corrections for the zero offset of the counter and the deviation of the sample surface from the focal plane of the diffractometer. The crystallographically oriented program Celsiz (version 1.1.6) [8] was applied for calculations which employs the least-squares method using the Miller indices hkl of the observed reflections. Microstructure parameters (average size D of crystallites, also called coherent scattering regions (CSR) of X-ray radiation, and absolute values of average microstrains ε_s in them) were estimated from diffraction patterns based on the full widths of the observed reflections at half the maximum of their intensity (FWHM, full width at half maximum) using the method of (crystallite)size — (micro)strain plot [9]. The procedures for the observed type of reflections (pseudo-Vogt type) were applied for the calculations using SizeCr program (version 11.04) [10].

The Vickers microhardness (H_V) of the samples was determined using tester PMT-3 with microscope AxioVert. A1 with Carl Zeiss Axiocam 208 digital optics. The imprints were obtained using a Vickers pyramid at a load of 1.96 N and with an exposure time of 10 s.

Samples with a rectangular section of $1.4 \times 2.5\,mm^2$ with a length of 25 mm were made from the central part of round start rods for acoustic studies.

Elastic and microplastic properties (Young's modulus E, amplitude-independent elastic vibration decrement δ, microplastic flow stress σ and inelastic strain ε_d) were studied using the resonance method of a composite piezoelectric vibrator like in Ref. [4]. The tests were carried out at a frequency of approximately 100 kHz in a wide range of oscillatory deformation amplitudes ε, including linear (amplitude-independent) and nonlinear (microplastic) regions. The formulas required for processing experimental data are given in Ref. [4]. The error of calculation of the modulus E of the sample was approximately 0.4%, the error of calculation of amplitude ε, decrement δ, stress σ and deformation ε_d was approximately 5%.

The density of the samples was determined by hydrostatic weighing using analytical balance Shimadzu AUW 120D (Shimadzu Corporation, Japan) with specific gravity measurement kit SMC-301. The relative error of determining the density is maximum 0.02%.

A more detailed description of the details of the experiment and analysis of acoustic and densitometric measurements by EBSD, XRD methods can be found in Ref. [11].

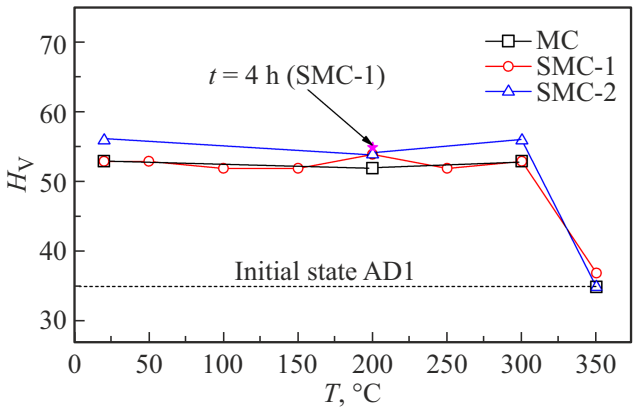

Figure 1. Dependence of microhardness H_V on annealing temperature for aluminum AD1 — MC, SMC-1 and SMC-2). Annealing duration is 45 min. The dotted line shows the microhardness value for the initial state AD1 (state of the delivery).

3. Experimental results

3.1. Microhardness

The simplest method to obtain preliminary data on the effect of temperature on mechanical properties is to study microhardness. Taking into account that the grain size d and hardness H_V are related by the empirical Hall–Petch relationship [12]:

$$H_V = H_0 + K_H d^{-1/2},$$

where K_H — the Hall-Petch coefficient, and H_0 corresponds to the hardness of a single crystal, first the temperature can be assessed at which there are changes in the physical (and structural) properties of the material. Microhardness was determined on samples after annealing with a step of 50°C. Figure 1 shows the dependences of the microhardness H_V on the annealing temperature for aluminum for three structural states. It was found that the microhardness value of all samples remains practically unchanged up to 300°C. The highest value of H_V is typical for the SMC-2 state. The increase of the annealing temperature to 350°C results to its significant decrease — by 1.4 times, the microhardness value becomes the same for all samples — 35. The increase of the annealing time to 4 h (at temperature 200°C, SMC-1) had little effect on the microhardness value; the increase was 1.9%.

3.2. Elastic and microplastic properties

The elastic and microplastic properties were determined after isothermal annealing at temperatures of 100, 200 and 300°C for a duration of 45 min in various structural states for studying the thermal stability of the studied aluminum AD1.

As an example, Figure 2, *a* and *b* show the amplitude dependences of the Young's modulus E and decrement δ,

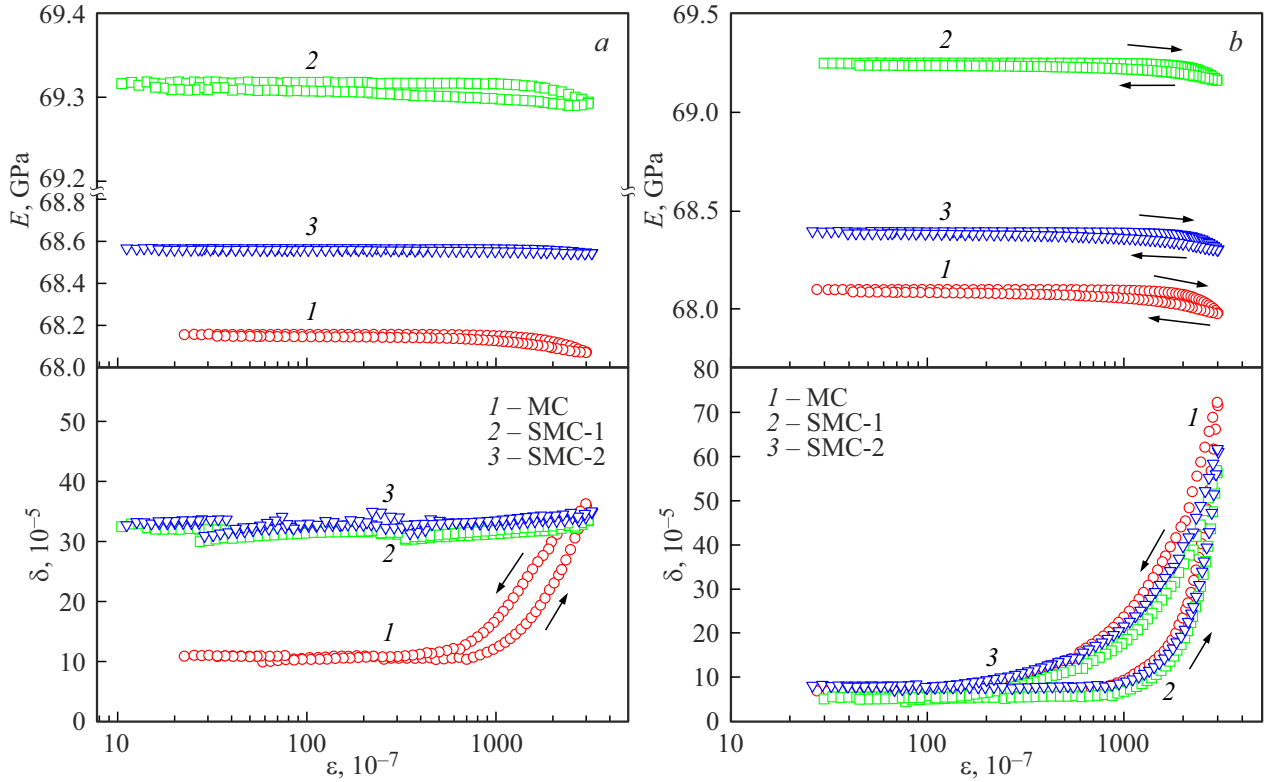

Figure 2. Amplitude dependences of Young's modulus E and decrement δ for aluminum samples AD-1, annealed at a — 100 and b — 300°C. Measurements were performed at room temperature.

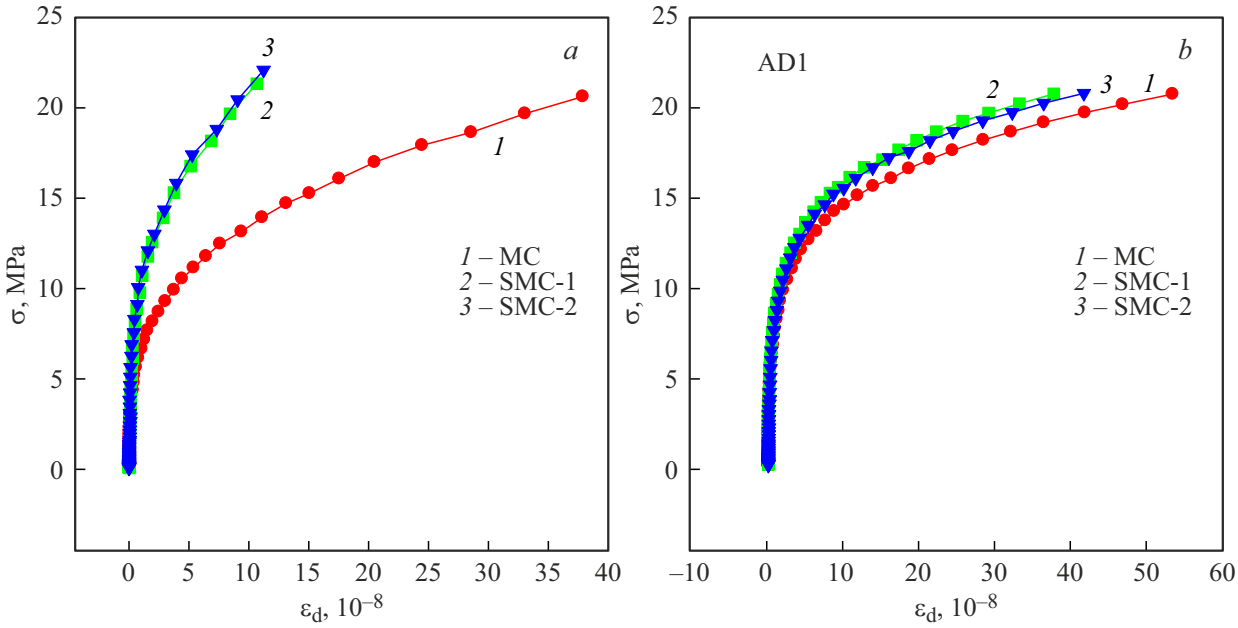

Figure 3. Diagrams of microplastic deformation of aluminum samples AD-1 after annealing at a — 100 and b — 300°C. Measurements were performed at room temperature.

and Figure 3, a and b shows the acoustic deformation diagrams of $\sigma(\varepsilon_d)$ after annealing at 100 and 300°C.

The comparison of the experimental data in Figures 2 and 3 demonstrates that an increase of the annealing temperature has virtually no effect on the modulus E. δ and σ change most noticeably for samples SMC-1 and SMC-2. The nature of the dependences of decrement $\delta(\varepsilon)$ and microplastic flow stress $\sigma(\varepsilon_d)$ and their absolute values

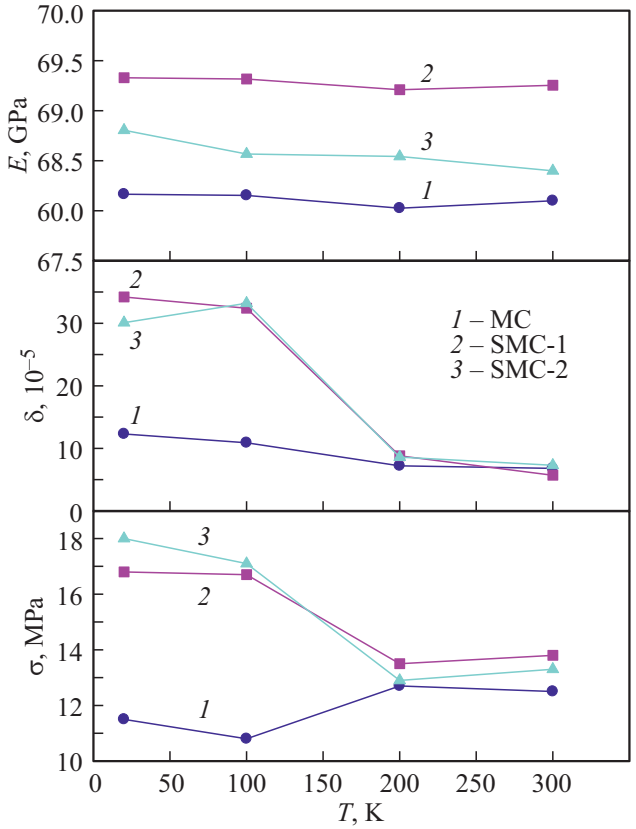

Figure 4. The effect of the annealing temperature T on Young's modulus E, amplitude-independent decrement δ and microfluidity stress σ during inelastic deformation $\varepsilon_d = 5.0 \cdot 10^{-8}$ for aluminum samples AD-1. Measurements were performed at room temperature.

in these samples with a temperature increase become close to the data for the sample in the MC state.

Figure 4 shows the dependences of the modulus E, amplitude-independent decrement δ and microfluidity stress σ (at $\varepsilon_d = 5.0 \cdot 10^{-8}$) on the annealing temperature. The figure shows that there is quite good stability of the modulus with the increase of the annealing temperature (there is only a slight decrease for SMC-2 and a slight increase to 300°C for MC and SMC-1), and δ and σ for SMC-1 and SMC-2 noticeably decrease and have close values after annealing at 200°C. It should be noted that the increase of the annealing temperature from 200 to 300°C did not significantly affect the further change of the elastic and microplastic properties.

3.3. Studies of grain structure (scanning-electron microscopy)

The results of the studies of the grain structure of AD1 before isothermal annealing are presented in Ref. [4]. It was shown that in the transverse section (perpendicular to the rolling direction) before annealing, the grains have an equiaxed appearance with average values of 1500, 470 and 500 nm for the MC, SMC-1 and SMC-2 states, respectively. The grains have a somewhat elongated shape in the rolling direction. No noticeable changes of the shape and size of the grain structure of AD1 (as in the study of mechanical, elastic and microplastic properties) were found after annealing in the temperature range 50–150°C according to the results of EBSD studies. Therefore, the structural data after annealing at temperatures of 200 and 300°C in the longitudinal section are mainly given below.

The characteristic distributions of grain sizes and grain boundaries by disorientation after annealing at 200°C for the SMC-1 state are shown in Figure 5 (longitudinal section), and in Figure 6 Euler maps before and after annealing at 200, 300 and 350°C.

It follows from the comparison of the previously obtained data (before annealing) [4] and Figures 5 and 6 that the grain structure of the sample remains quite stable (up to 200°C inclusive). The annealing in the range up to 200°C also did not result in noticeable changes in the structure for other states — SMC-2 and MC. After annealing at a temperature of 300°C, according to scanning-electron microscopy data, the structure for all three states (MC, SMC-1 and SMC-2) is represented by equiaxed grains, the size of which varies in the range 10–12 μm, which is a consequence of the process of collective recrystallization. These data are quite consistent with the fact that $T = 300$°C is noticeably higher than the temperature $0.25T_{\text{melt}}$, at which the recrystallization process begins for most commercially pure metals. It was shown in [13] that the UFG structure of aluminum alloys, formed by the method of equal channel angular pressing, is also preserved at a temperature of up to 200°C (for example, for the Al 1100 alloy, the composition of which is close to the AD1 alloy).

The distribution of grain boundaries by disorientation (Figure 5) showed that small-angle boundaries predominate in the central part of the rod with a small peak at the disorientation angle 55°. The proportion of boundaries with large disorientations increases closer to the edge of the rod (with disorientation angles greater than 15°) and the proportion of boundaries with disorientations approximately 55° remains the same as in the central part. No noticeable changes of the distributions along grain boundaries after annealing at 200°C (in comparison with the samples before annealing [4]) were found.

3.4. X-ray diffraction studies

The characteristic form of the measured X-ray diffraction patterns is shown in Figure 7 using the example of X-ray diffraction patterns obtained from a MC sample before and after annealing in air at 200°C.

According to the obtained diffraction patterns, the samples in MC and SMC-1 before annealing showed a predominant orientation along the [001] and [011] directions, respectively (in contrast to Al without the effects of preferential orientation, where the reflection 111 is most

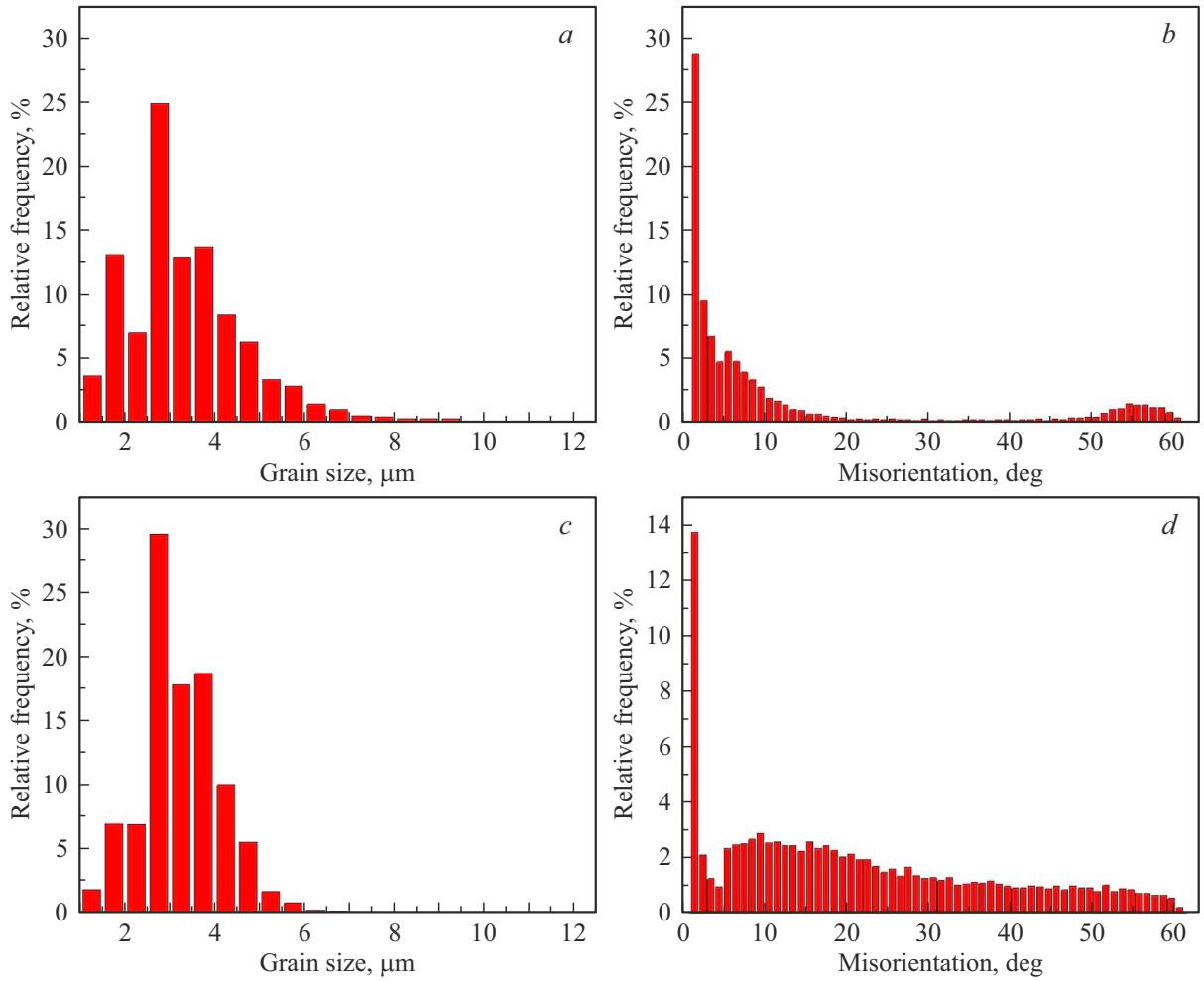

Figure 5. Microstructure of aluminum alloy AD1 (SMC-1) — distribution of grain sizes and disorientation angles of grain boundaries in the center (a, b) and edge (c, d) rod after annealing at $T = 200°C$.

intensive and approximately half as large — reflection 002, see PDF-2 map 00-004-0787). The predominant orientation along [001] in the SMC-1 sample after annealing at 200°C is the same as before annealing. A predominant orientation along [001] began to develop in the MC and SMC-2 samples after annealing.

The formation of a new reflection with the Bragg angle $2\theta_B \approx 32°$ (Figure 8) is another consequence of annealing in air, visible in the measured diffraction patterns, which can be attributed to one of the modifications Al_2O_3 (reflection 020 δ-Al_2O_3, or 220 δ^*-Al_2O_3, or -401 θ-Al_2O_3 according to PDF-2 maps 00-046-1131, 00-046-1215 and 01-086-1410 respectively). The intensity of the reflection formed after annealing and attributed to Al_2O_3 is maximum in the sample MC and minimum in SMC-2. An approximate estimate made by simulating the intensity ratio of the observed reflection Al_2O_3 (one of the potential oxides, θ-Al_2O_3 is taken as an example (PDF-2 map 01-086-1410), then this is the reflection -401) and the reflection 002 Al using the program Powdercel (version 2.4) [14] gives the Al_2O_3 weight content ~ 5.8 wt% for the MC sample after 200°C annealing and ~ 2.9 and 2.0 wt% in annealed at 200°C samples SMC-1 and SMC-2 respectively.

Before annealing, Al reflections with the same indices shift towards smaller Bragg angles from the sample SMC-1 to SMC-2 and MC (Figure 9 as an example), i. e., based on from Bragg's law, the parameter a of the cubic unit cell Al of the material of sample SMC-1 is greater than that of sample SMC-2, and, in turn, that of sample SMC-2 is greater, than MC. A shift of the Bragg angles of the reflections to larger values for all samples is observed after annealing, i. e. parameters a of Al material decreases in all samples. However, the tendency for the parameter a to increase from sample SMC-1 to SMC-2 and further to MC persists, as can be judged by the position of the reflections (Figure 9). Quantitative calculations of the parameter a of the material of the Al samples confirm these preliminary observations (see table).

No microstrains were observed in the Al crystallites of the MC and SMC-2 samples either before or after annealing according to the data presented in the table. The annealing results in the growth of crystallites (see the table) for all structural states. Microstrain $\varepsilon_s = 0.011\%$ was found

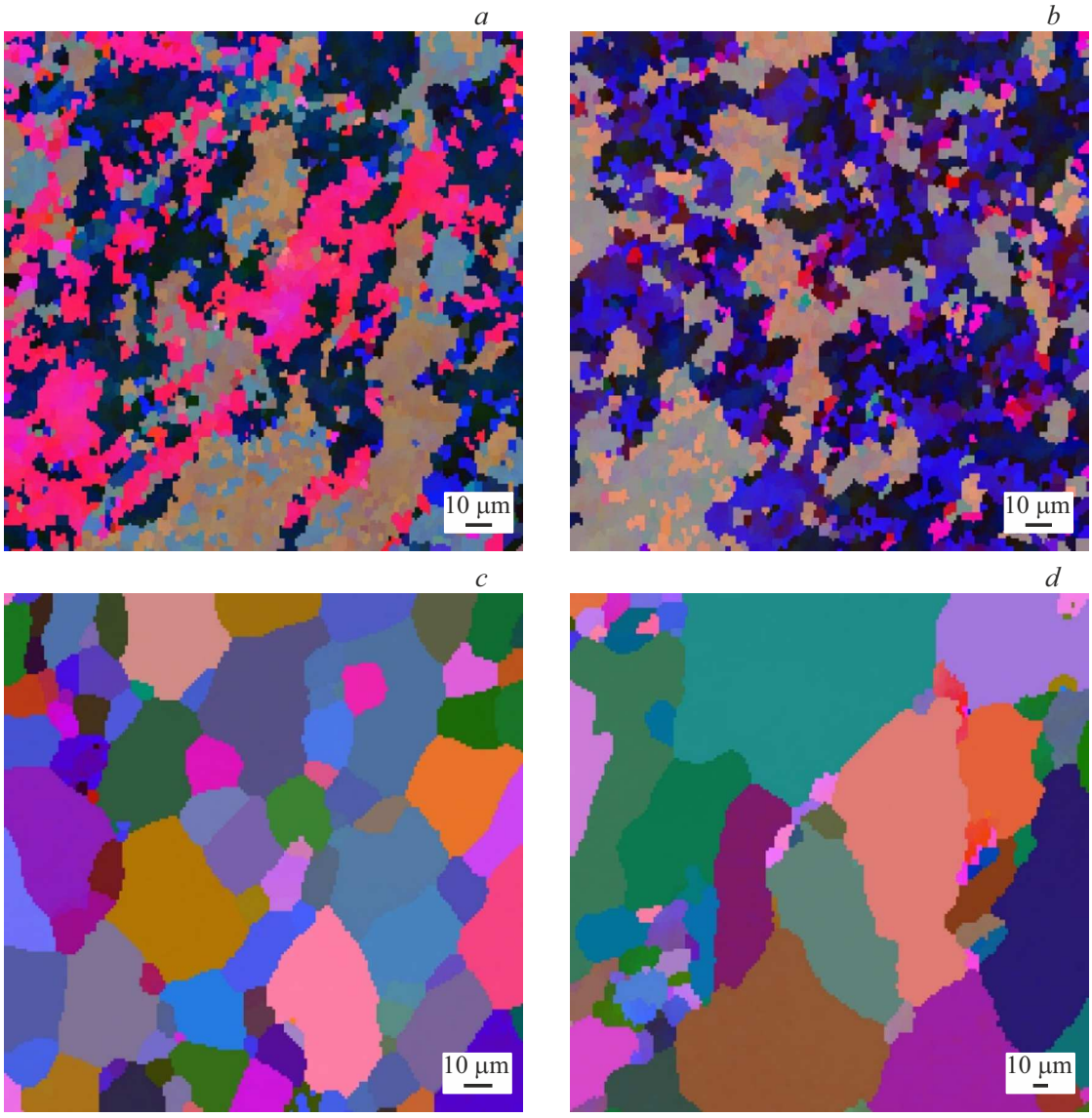

Figure 6. Euler maps for AD1 SMC-1 states: before annealing (*a*), annealing at 200°C (*b*), annealing at 300°C (*c*), annealing at 350°C (*d*).

in the SMC-1 sample before annealing. After annealing, microstrain disappears ($\varepsilon_s = 0$), the average Al crystallite size decreases from 184 nm before annealing to 170 nm after annealing.

Parameter a of the cubic lattice cell of the material of Al samples, the average size D of crystallites and the microstrain ε_s in them (temperature during measurements 41 ± 1°C)

Sample	a, Å	D, nm	ε_s, %
MC	4.05131±0.00030	131.1±8.4	0
SMC-1	4.04933±0.00011	183.8±9.2	0.011±0.003
SMC-2	4.05035±0.00030	194.2±8.4	0
MC (200°C)	4.05035±0.00010	157±17	0
SMC-1 (200°C)	4.04917±0.00007	170±15	0
SMC-2 (200°C)	4.04919±0.00040	216±10	0

4. Discussion

Let us analyze changes in microhardness, elastic and microplastic properties during annealing, taking into account structural studies. The microhardness value at 20°C is almost 10% higher for the SMC-2 sample than for the MC and SMC-1 states. This is attributable to the peculiarity of deformation at low temperatures, which contribute to the formation of a smaller grain size and a significant increase of dislocation density. For instance, the use of cryotemperature in [15] under the same plastic deformation modes resulted in an increase of the dislocation density by 2.25 times and an increase of the microhardness H_V to 4%. H_V virtually does not change for all samples in case of annealing temperature of to 150°C. An increase of the annealing temperature for the SMC-1 sample resulted in an increase of microhardness by 3.8% (data for $T = 200$°C). It is known that the

annealing leads to relaxation of internal stresses for most UFG materials, which also affects microhardness. The most likely reason for the anomalous increase of microhardness is an increase of the density of lattice dislocations [16]. The authors [16] observed a similar effect for the submicro- and nanocrystalline states of aluminum alloys, where the increase of the microhardness was found at the annealing temperature of 200°C for the alloy Al-3% Mg and 300°C for the alloy Al 1570. It should be noted that a decrease of the parameter of the cubic lattice cell of the samples was found (see the table) at $T = 200$°C, which may indirectly indicate an increase of the concentration of impurity atoms in the volume of grains during the dissolution of precipitate particles at grain boundaries [16]. The same reason explains the stability of microhardness for sample SMC-2. It is obvious that annealing at 350°C forms a coarse-grained

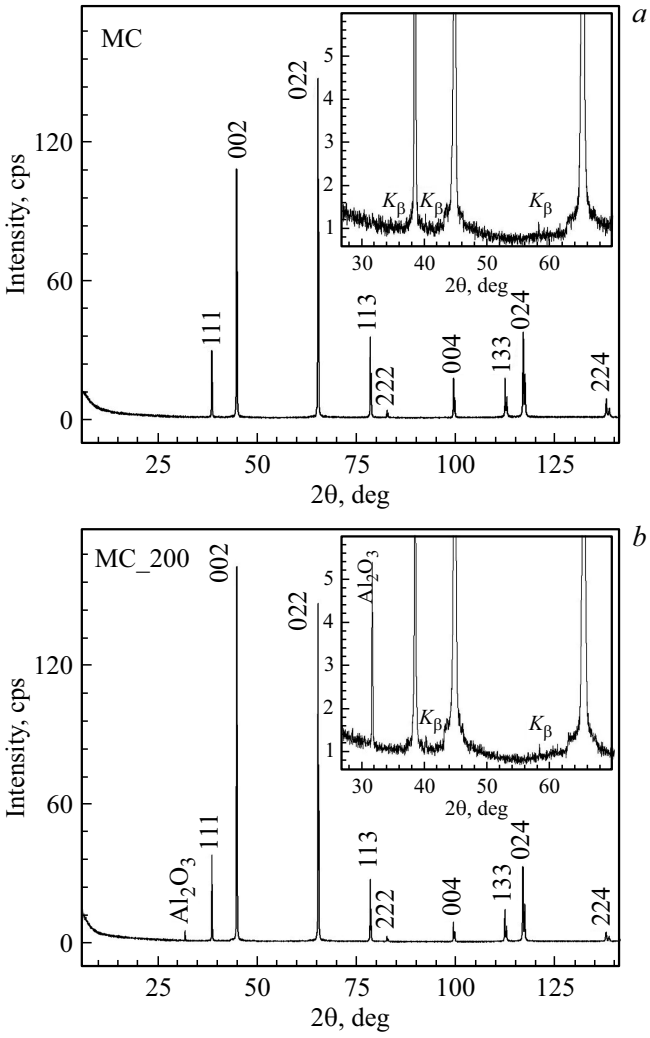

Figure 7. XRD patterns of the MC sample before (a) and after (b) annealing in air at 200°C. Miller indices hkl of the observed Al XRD reflections are shown. A reflection that belongs to one of the modifications of Al_2O_3 is shown on (b). The insets in (a) and (b) show the range of diffraction angles $2\theta = 27-70^\circ$ on an enlarged scale. K_β — remnants of reflections corresponding to K_β radiation. Temperature during the measurements is 41 ± 1°C.

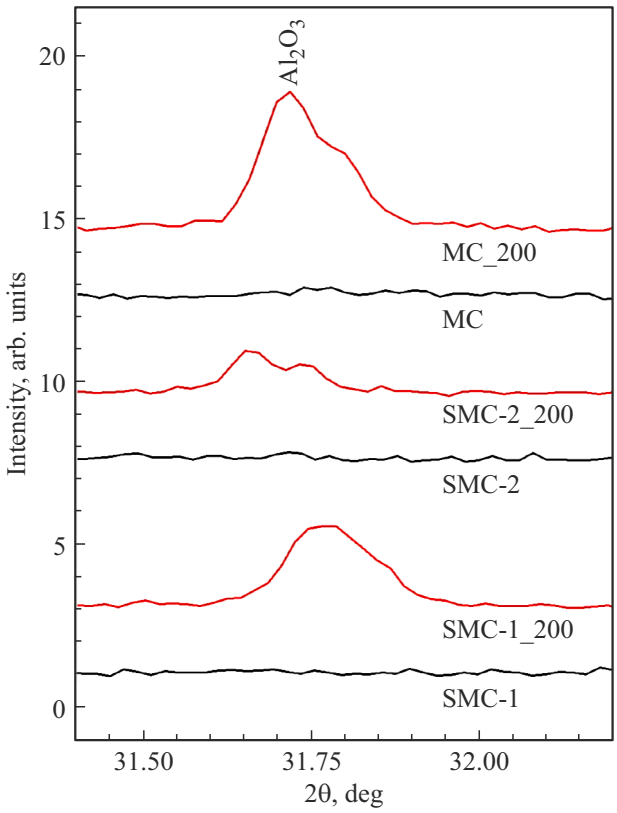

Figure 8. Part of the XRD patterns of the measured samples in the diffraction angle range 2θ, within which a reflection is formed, attributed to one of the modifications Al_2O_3 after annealing in air at 200°C. For convenience, the XRD patterns are shifted along the vertical axis. Temperature during the measurements is 41 ± 1°C.

equilibrium state (Figure 6) for all samples and the value of H_V corresponds to the microhardness value for the initial state AD1 (as delivered), Figure 1.

It is convenient to use the data in Figure 4 for the analysis of changes of elastic and microplastic properties in different structural states, which shows the dependences of the Young's modulus, decrement and stress of microplastic flow on the annealing temperature.

The reasons influencing the noticeable difference of the Young's modulus before annealing were considered in Ref. [4]. For instance, it was shown that the higher value E for SMC-1 is attributable (primarily) to the impact of high internal stresses. This is confirmed by XRD studies in this paper, according to which the value of microstrain ε_s is different from zero only in this sample and amounts to 0.011%, which should result in an increase of internal stresses. The annealing is actually the transition from liquid nitrogen temperature to 20°C (after rolling) for the SMC-2 sample [17], and, therefore, such post-deformation heating to room temperature can be considered as „annealing", which results in a more equilibrium state and a decrease of the level of internal stresses. This also explains the lower value of modulus E for MC aluminum, the structural state of which was obtained by post-deformation annealing, compared to samples SMC-1 and SMC-2.

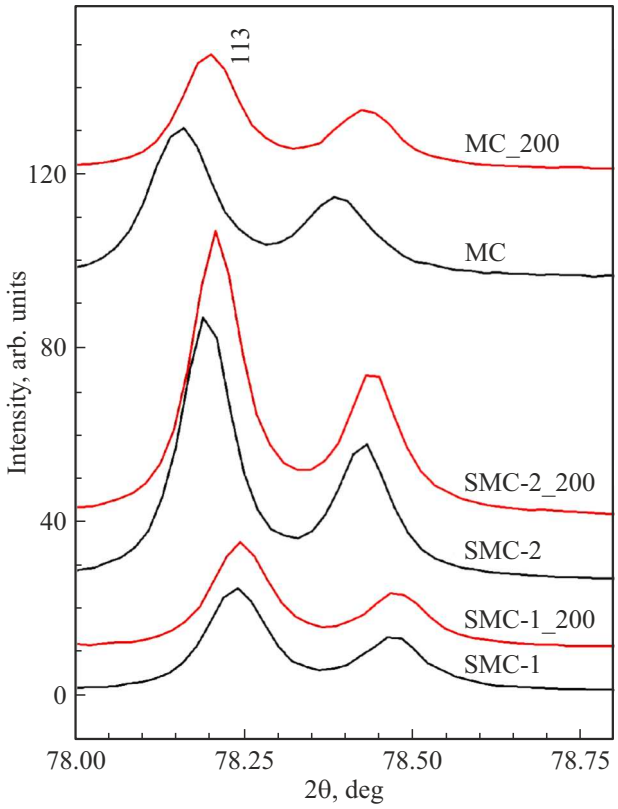

Figure 9. Part of the XRD patterns of measured samples near the Al reflection with Miller indices $hkl = 113$. For convenience, the XRD patterns are shifted along the vertical axis. Temperature during the measurements 41 ± 1○C.

After additional annealing the values of the Young's modulus of each sample change a little as follows from Figure 4. A slight increase is observed at 300°C for SMC-1 and MC. The formation of oxides Al_2O_3 on the surface of the samples after annealing was found by using the XRD method. The modulus of elasticity Al_2O_3 is 365−393 GPa according to the data [18]. Estimates showed that the largest weight fraction of Al_2O_3 is characteristic of the MC sample (~ 5.8 wt%), and the modulus value for this sample remains the smallest. It can be assumed that the occurrence of the Al_2O_3 layer after annealing of the MC sample, and even more so of the SMC-1 and SMC-2 samples, characterized by an even smaller weight fraction of Al_2O_3, does not have a significant effect on the modulus value.

The value of the decrement δ significantly changes in contrast to the Young's modulus. Different decrement values for the SMC-1, SMC-2 and MC states before annealing were discussed in Ref. [4]. The increase of crystallite sizes is observed for all structural states after annealing at 200°C according to the table (i.e. CSR — „perfect crystal" region). Apparently, the number of mobile dislocations in crystallites becomes smaller, which should lead to a noticeable decrease of the decrement.

It should be noted when reviewing the data presented in Figures 2, *b* and 3, *b* that the behavior of the dependences of decrement $\delta(\varepsilon)$ and voltage $\sigma(\varepsilon_\delta)$ after annealing at 300°C becomes almost the same for all three aluminum samples. Identical dependences are a consequence of the formation of the same structural state due to collective recrystallization (which is confirmed by structural studies carried out using electron microscopy methods — Figures 5 and 6).

The amplitude hysteresis of the $\delta(\varepsilon)$ curves (Figure 2, *b*) is most likely associated with the mobility (reorientation) of dislocation pinning centers during the measurement of the amplitude dependence. Such stoppers can be either impurities or dispersed particles, the presence of which was detected at high magnifications in a transmission electron microscope on a sample of MC aluminum. The dispersed particles are oxides aluminum and copper according to energy-dispersive X-ray spectroscopy [19].

5. Conclusion

The formation of an ultra-fine grain structure in technical aluminum AD1 results in a significant change of elastic and microplastic properties. This work found a fairly high thermal stability of the grain structure in the SMC-1 and SMC-2 states up to a temperature of 200°C, and microhardness and modulus of elasticity at a temperature of up to 300°C. The crystalline Al_2O_3 (up to ~ 5.8 wt%) formed during annealing in air does not have a noticeable effect on the value of the Young's modulus E of technical aluminum AD1. As the size of Al crystallites increases after annealing, the decrement δ significantly decreases — apparently due to a decrease of the number of mobile dislocations.

Acknowledgments

The authors express their gratitude to Yu.R. Kolobov for providing AD1 aluminum samples. Structural studies were carried out using the equipment and software of the Common Use Center „Materials Science and Diagnostics in Advanced Technologies" (Ioffe Institute, St. Petersburg).

Conflict of interest

The authors declare that they have no conflict of interest.

References

[1] K. Edalati, A. Bachmaier, V.A. Beloshenko Y. Beygelzimer, V.D. Blank, W.J. Botta, K. Bryła, J. Čížek, S. Divinski, N.A. Enikeev, Y. Estrin, G. Faraji, R.B. Figueiredo, M. Fuji, T. Furuta, T. Grosdidier, J. Gubicza, A. Hohenwarter, Z. Horita, J. Huot, Y. Ikoma, M. Janeček, M. Kawasaki, P. Král, S. Kuramoto, T.G. Langdon, D.R. Leiva, V.I. Levitas, A. Mazilkin, M. Mito, H. Miyamoto, T. Nishizaki, R. Pippan, V.V. Popov, E.N. Popova, G. Purcek, O. Renk, Á. Révész, X. Sauvage, V. Sklenicka, W. Skrotzki, B.B. Straumal, S. Suwas, L.S. Toth, N. Tsuji, R.Z. Valiev, G. Wilde, M.J. Zehetbauer, X. Zhu. Mater. Res. Lett. **10**, *4*, 163 (2022). https://doi.org/10.1080/21663831.2022.2029779

[2] S.V. Dobatkin. Tekhnologiya legkikh splavov *3*, 5 (2011). (in Russian).
[3] M. Eizadjou, H.D. Manesh, K. Janghorban. J. Alloys. Compound **474**, *1–2*, 406 (2009).
[4] [M.V. Narykova, B.K. Kardashev, V.I. Betekhtin, A.G. Kadomtsev, A.I. Lihachev, O.V. Amosova. Phys. Solid State **65**, *8*, 1326 (2023).
[5] M.B. Ivanov, A.V. Penkin, Y.R. Kolobov, E.V. Golos, D.A. Nechayenko, S.A. Bozhko. Deformatsiya i razrushenie materialov *9*, 13 (2010). (in Russian).
[6] Bruker AXS. Karlsruhe, Diffrac. Suite Eva Version 5.1.0.5; DIFFRAC.SUITE User Manual; Bruker AXS GmbH: Karlsruhe, Germany (2019).
[7] International Centre for Diffraction Data (ICDD). Powder Diffraction File-2Release 2014. ICDD: Newton Square, PA, USA (2014).
[8] C. Maunders, J. Etheridge, N. Wright, H.J. Whitfield. Acta Cryst. B **61**, *Part 2*, 154 (2005).
[9] B. Terlan, A.A. Levin, F. Börrnert, F. Simon, M. Oschatz, M. Schmidt, R. Cardoso-Gil, T. Lorenz, I.A. Baburin, J.-O. Joswig, A. Eychmüller. Chem. Mater. **27**, *14*, 5106 (2015).
[10] A.A. Levin. Program SizeCr for calculation of the microstructure parameters from X-ray diffraction data, preprint (https://www.researchgate.net/profile/Alexander-Levin-6/research) (accessed on 5 June 2022). https://doi.org/10.13140/RG.2.2.15922.89280
[11] M.V. Narykova, A.A. Levin, N.D. Prasolov, A.I. Lihachev, B.K. Kardashev, A.G. Kadomtsev, A.G. Panfilov, R.V. Sokolov, P.N. Brunkov, M.M. Sultanov, V.N. Kuryanov, V.N. Tyshkevich. Crystals **12**, *2*, 166 (2022). https://doi.org/10.3390/cryst12020166
[12] E.O. Hall. Proc. Phys. Soc. B **64**, *9*, 747 (1951).
[13] Z. Horita, T. Fujinami, M. Nemoto, T.G. Langdon. Mater. Proc. Technol. **117**, *3*, 288 (2001).
[14] W. Kraus, G. Nolze. J. Appl. Cryst. **29**, *Part 3*, 301 (1996). https://doi.org/10.1107/S0021889895014920
[15] H. Xiong, Y. Zhou, P. Yang, C. Kong, H. Yu. Mater. Sci. Eng. A **853**, 143764 (2022). https://doi.org/10.1016/j.msea.2022.143764
[16] N.K. Tsenev, V.N. Perevezentsev, M.Yu. Shcherban', A.N. Tsenev. Tech. Phys. **55**, *6*, 822 (2010).
[17] P.A. Khaimovich. Fizika nizkikh temperatur **44**,*5*, 463 (2018). (in Russian).
[18] Springer handbook of condensed and materials data / Eds W. Martienssen, H. Warlimont. Berlin, Springer (2005). 1119 p.
[19] S.S. Manohin, V.I. Betekhtin, A.G. Kadomtsev, M.V. Narykova, O.V. Amosova, Yu.R. Kolobov, D.V. Lazarev. Phys. Solid State **65**, *1*, 126 (2023).

Translated by A.Akhtyamov